Journal of Geophysical Research, Space Physics Vol. 75, No. 16, June 1, 1970

Pioneer 8 Electric Field Measurements in the Distant Geomagnetic Tail

F. L. Scarf and I. M. Green

Space Sciences Laboratory, TRW Systems Group, Redondo Beach, California 90278

G. L. Siscoe

Department of Meteorology, University of California, Los Angeles, California 90024

D. S. Intriligator,[1] D. D. McKibbin, and J. H. Wolfe

Space Science Division, NASA Ames Research Center, Moffett Field, California 94035

The Pioneer 8 space probe encountered the extension of the earth's magnetic tail in January of 1968, at downstream distances of 500–800 R_E. During this period the VLF electric field experiment sporadically detected some characteristic changes in the plasma wave noise spectrum that appeared in close association with tail-like positive ion energy spectra. In this report, we correlate the Pioneer 8 wave and particle observations in detail and show that during the extended tail crossings the average broadband wave levels were reduced. Enhanced 400-Hz activity was frequently detected near the tail boundaries, however, and the observations suggest that tail breakup and field-line reconnection phenomena begin to be important within 500 R_E.

Introduction

The geomagnetic tail contains one of the few natural plasma configurations that allows the stability of a current pinch or neutral sheet to be investigated directly over long time periods. A number of spacecraft have carried instrumentation to measure tail-associated phenomena out to lunar orbit; only the two probes Pioneers 7 and 8, however, have directly traversed the geomagnetic tail and wake regions at downstream distances of 500–1000 R_E. In September of 1966, Pioneer 7 passed through the anticipated tail region with $X_{SE} \simeq -800$ to -1050 R_E, and $Z_{SE} \simeq 25$ to 29 R_E (the *SE* subscripts refer to solar ecliptic coordinates). During this period the ARC electrostatic analyzer intermittently detected very disturbed positive ion spectra, with occasional flux decreases down to the level of instrument sensitivity [*Wolfe et al.*, 1967]. The plasma probe experimenters described this region as a geomagnetospheric wake, and *Ness et al.* [1967] demonstrated that many magnetic features could be related to multiple encounters with the distant geomagnetic tail.

The Pioneer 8 probe, launched on December 13, 1967, had a trajectory specifically designed to pass through the expected tail region at a smaller downstream distance, and on January 23, 1968, the spacecraft solar ecliptic coordinates were $X_{SE} = -525$ R_E, and $Z_{SE} = 10.5$ R_E, with a probe-sun-earth angle of 5.5°. The 5.5° deviation from the anti-solar direction is approximately equal to the value expected for tail aberration with a wind speed near 400 km/sec, and thus Pioneer 8 was in a good position to observe tail or wake effects for a considerable time interval centered about January 22–23, 1968.

The Pioneer 8 plasma probe again found that intervals of quiescent plasma ion energy spectra were interrupted by periods with abrupt changes in the magnitude and shape of the spectra, or by periods with complete absence of measurable plasma [*Intriligator et al.*, 1969]. The Pioneer 8 magnetometer observations suggested detection of tail characteristics similar to those observed

[1] Present address, Department of Physics, California Institute of Technology, Pasadena, California 91109.

on Pioneer 7, but for a higher percentage of the time [*Mariani and Ness*, 1969]. In this note we extend the discussion of the Pioneer 8 tail crossing by reporting on the VLF plasma wave observations made with the electric field experiment on the spacecraft.

It is natural to be concerned with the excitation of waves in this region for a number of reasons. The ARC observations reveal that the plasma spectra are frequently non-Maxwellian and that the bulk parameters are highly nonuniform; these characteristics imply that some wave-particle interactions or plasma instabilities are operative. If reconnection and field annihilation phenomena occur in the distant tail, then wave excitation also provides a natural dissipation mechanism [e.g., *Axford*, 1967; *Dungey*, 1969; *Dungey and Speiser*, 1969]. Ideally, wave measurements should be available over a broad frequency range, because there are many conceptual possibilities for wave-particle interactions, and a complete assessment of the dynamical situation requires observations of all oscillation modes. However, the Pioneer 8 electric field experiment described by *Scarf et al.* [1968] is quite rudimentary, and in the tail region only the qualitative broadband channel and the 400-Hz bandpass channel have physically significant response.

In the following sections we discuss some aspects of the VLF electric field observations for the period extending from January 1 through February 15, 1968, and we compare wave data with plasma and magnetic field observations. The emphasis here is on the tail crossings; in a forthcoming paper [*Siscoe et al.*, 1970*a*] evidence suggesting that a geomagnetic wake extends to (500–700) R_E downstream is separately discussed.

The basic results described here can be summarized as follows. (*a*) There are many intervals in the downstream region where the electric field wave spectrum differs markedly from the conventional interplanetary forms. (*b*) An identification of tail-affected intervals based on the occurrence of changes in the plasma energy spectrum is generally consistent with an identification based on variations in the wave spectrum. (*c*) Enhanced 400-Hz wave activity is frequently detected near the boundaries where rapid changes in magnetic field magnitude and direction are also found. These sporadic events sometimes resemble the OGO 5 wave-field interactions found near *X*-type nulls [*Scarf et al.*, 1969], and we conjecture that field line merging occurs at 500–800 R_E, with the VLF electric field oscillations leading to significant dissipation.

Broadband E Field Characteristics

The sixteen Pioneer 8 broadband channels provide a pulse-height analysis of the composite waveform that includes the ambient signal and local noise. The overall frequency sensitivity range extends from 100 Hz to 100 kHz, but, for sufficiently weak external signals with $0.1 \lesssim f \lesssim$ 1–5 kHz, the response is relatively independent of ambient frequency, as is shown in Figure 4 of *Scarf et al.* [1968]. If the spectral form remains constant, the broadband output then gives a qualitative measure of the external signal amplitude. As in the past, we assume that the spectrum has this shape, and here we display the response to an equivalent 100-Hz sine wave. At the 512-bits/sec telemetry rate used in January and February of 1968, the broadband scan cycle was repeated every 7.46 min.

It is useful to group the broadband readings in hourly sequences and to plot the maximum and minimum values in each group. Broadband data for the period December 15, 1967, through May 5, 1968, were displayed in this format in a recent review by *Scarf* [1969], and a comprehensive discussion of the Pioneer 8 interplanetary results, covering 10 solar rotations, is now in preparation. In this report, concerned with the distant geomagnetic tail, we first focus attention on the time interval extending from January 9 through February 1, 1968.

Figure 1 shows the hourly maximum-minimum values for the broadband response, with hourly data samples for several other parameters. The peak velocity is the speed of a proton with streaming energy corresponding to the maximum cold beam equivalent flux; this peak velocity is defined by a best fit procedure involving three adjacent energy channels, as described by *Intriligator et al.* [1969]. When the thermal energy of the wind is small compared with the streaming speed, the peak velocity is a good approximation to the true streaming speed. For normal solar wind conditions, the peak velocities will run slightly higher (by 5–10%) than the true wind speeds, and it is convenient to neglect

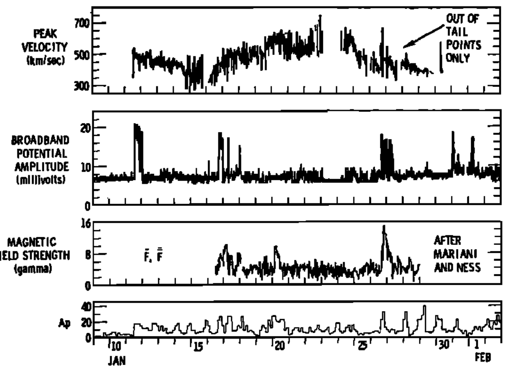

Fig. 1. Hourly maximum and minimum values for representative particle, field, and wave parameters, measured when Pioneer 8 traversed the expected location of the extended geomagnetic tail. The peak wind velocity is defined by a best-fit procedure involving three adjacent energy channels; during the January 11–30 period the data are shown only for E/Q spectra that have been judged to be out-of-tail. The broadband electric field amplitudes are qualitative indicators of the VLF activity for $f > 100$ Hz, and all measured points are shown. The magnetic field strength values are taken from the report by *Mariani and Ness* [1969], and two variables ($\langle F \rangle$ and $\langle \bar{F} \rangle$) are plotted on the same scale. Here $\langle F \rangle$ and $\langle \bar{F} \rangle$ refer to mean values obtained by different averaging techniques.

the thermal corrections. The magnetic field measurements are taken from the report by *Mariani and Ness* [1969]; here $\langle F \rangle$ and $\langle \bar{F} \rangle$ are hourly averages of the field magnitude obtained by different averaging methods.

The electric field amplitudes and the magnetic field strength values in Figure 1 represent all of the measurements for the intervals shown, but the plasma probe data are displayed only for those points that have been judged to be 'out of the tail.' The criteria used to decide that a given spectrum is 'in the tail' can roughly be described as the following. (1) If a plasma energy spectrum resembles any of the 'basic disturbed spectra' described by *Intriligator et al.* ([1969] see especially Figure 4), we call this tail. (2) If $j_{max} < 10^6$ ions/cm^2 sec, we call this tail. (3) If the angular distribution is highly erratic on a time scale compared with one plasma probe scan period (approximately 65 sec), we refer to this as tail.

The criteria have been applied by one of the authors (D.D.M.) in a program that included actual examination of every positive ion spectrum; all spectra for the January 12–28 period have been separated into in-tail and out-of-tail groups on the basis of the ARC plasma probe response. (More details of this grouping and of the selection procedures will appear in a forthcoming report on the size and orientation of the extended tail.) Between January 12 and 28, all open spaces in the plasma probe data of Figure 1 represent complete hours when no out-of-tail spectra were obtained. In addition, during all hours for which a portion of the readings represent in-tail ion spectra, the data displayed here include only the out-of-tail points.

Figure 1 shows the combined response of several plasma diagnostic instruments when various types of interplanetary events are encountered. Interplanetary shock fronts generally produce broadband noise, and the discontinuities at 1400 on January 11 and at 1600 on January 26 were clearly associated with specific sudden commencements on the earth. Sudden impulses also generally appear to be related to the passage of discontinuities and noise boundaries, and Figure 1 displays some of these events; for example, ground si's detected at 1947 on January 16, at 1320 on January 17, at 0912 on January 30, and at 1211 on February 1 can be associated with Pioneer 8 broadband noise bursts. Further discussion of interplanetary features appears elsewhere [*Scarf et al.*, 1968; *Scarf* 1969; *Siscoe et al.*, 1970*b*]; here we focus attention on the tail-related aspects of these observations.

The plasma flux and energy spectrum criteria described above clearly lead to tail identification for a number of lengthy periods. A prominent nearly continuous interval extends from early on January 23 to about midday on the 24th. Figure 1 also reveals that entire 1-hour periods with no out-of-tail plasma were detected as early as January 15 and as late as January 27. Thus, this grouping of data points for 1-hour intervals provides enough crude resolution to indicate where the main or longest tail crossings were made.

The magnetometer data show that the field strength generally remained fairly steady in this entire region, although some sizable gaps between $\langle F \rangle$ and $\langle \bar{F} \rangle$ suggest the presence of significant low-frequency electromagnetic noise; we refer to the report by *Mariani and Ness* [1969] for further discussion.

The VLF potential amplitude plot of Figure 1 shows some specific changes in the broadband response during the most prominent of the tail crossings. As noted above, it is assumed here that a 100-Hz sine wave is continuously being measured, and we see that the plasma probe data gap from early on January 23 to the middle of the 24th does correspond to a distinct decrease in the equivalent potential amplitude to 5.5 mv, the system background. Many other decreases to this level are clearly related to certain plasma probe data gaps (e.g., the gap late on the 15th and on the 19th and 25th), and Figure 1 does suggest that there is a specific relationship between the encounter with tail plasma and the appearance of very low equivalent broadband electric fields. This hourly max-min format can do no more than suggest such a relationship, however, because for any hours containing both in-tail and out-of-tail points the broadband minimum may be low for the in-tail period while the plasma parameters will be displayed for the out-of-tail period.

To proceed with a correlation analysis it is necessary to go beyond unphysical 1-hour selections and to formulate new categories that correspond to the plasma probe spectral characteristics. Figure 2 contains a low-resolution version of this regrouping, with a Pioneer 8 trajectory plot that indicates where the observations were made. The bottom box describes plasma probe data covering the period from January 12 through 28. For each 12-hour period in this interval, the gray shading indicates the percentage of time in which tail ion spectra were found. The first brief tail crossing found on the plasma probe data occurred near 0400 on January 12, as the solar wind flow direction became irregular some 16 hours after the January 11 shock was encountered (see Figure 3, *Scarf* [1969]). Pressure changes associated with the si events of January 16 and 17 must undoubtedly be considered when assessing the other early intervals of tail encounter, and the

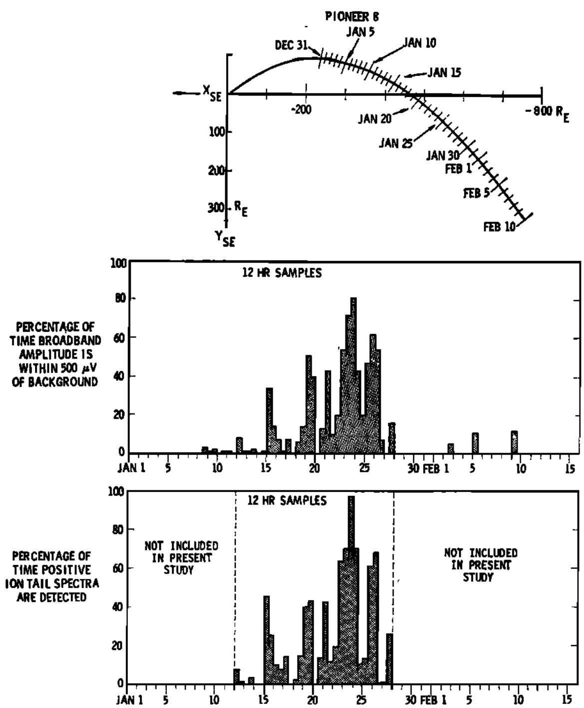

Fig. 2. Distribution of tail spectra and low broadband amplitude values. Top: projection of the Pioneer 8 near-earth trajectory in the ecliptic plane. For a 400-km/sec solar wind the aberration angle is 5.5°, and in this case the main tail crossing would be expected on January 23. Bottom panels: 12-hour percentage samples for occurrence of low broadband amplitudes and for the appearance of in-tail positive ion spectra, using the plasma probe criteria described in the text.

measurements on January 15–18 could also be affected by the proximity of a complex sector boundary [*Wilcox and Colburn*, 1969]. It is clear from the plasma data, however, that the main tail passage occurred during the January 22–26 interval, with a sharp drop in the probability of encounter following the storm at 1600 on January 26. It is not immediately evident why the distribution of tail encounter time has such a pronounced minimum from 1200 on the 24th to 1200 on the 25th, but Figure 1 does show that the plasma characteristics were quite variable during this time. At any rate, the indication that the January 22–26 period contains a large number of tail plasma spectra is consistent with the expectation that the extended geomagnetic tail should simply be aberrated from the antisolar direction.

The central box in Figure 2 contains a similar percentage plot for the broadband electric field measurement, constructed by tabulating all samples with $5.5 \leq \phi \leq 6$ mv. During the interval January 12–28 it is evident that the appearance of very low fields correlates well with the detection of tail ion spectra, at least on the basis of overall duration for each 12-hour interval. For the electric field plot we also extend the display to cover the period January 1 through February 15. It can be seen that very few readings with ϕ-ϕ(background) ≤ 500 μv were found beyond the January 12–28 period, and that no such low values were detected before January 8 or after February 9. The few isolated regions having low broadband values probably have some relation to the tail, but for extremely brief encounters it becomes difficult to determine with certainty that the positive ion spectra satisfy the in-tail criteria. For instance, the low noise region of February 2 was not clearly associated with an in-tail ion spectrum, but on February 5 the encounter was of sufficient duration to be detectable in the plasma probe data. We conclude that the very low broadband readings are only found in the neighborhood of the extended geomagnetic tail, and that the time duration of the tail crossing can be determined equally well from the electric field detector response or from the plasma probe spectral analysis.

The two distributions of Figure 2 are not actually identical, and this suggests the need for an additional correlation study conducted

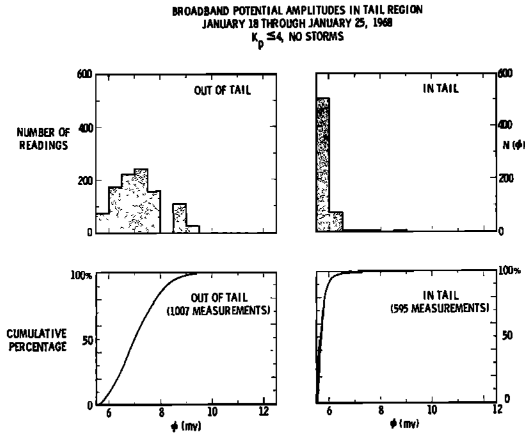

Fig. 3. High resolution comparison of in-tail and out-of-tail potential amplitude distributions.

with the highest possible temporal resolution. Accordingly, the distributions of Figure 3 were prepared by using two distinct groups of time sequences for the broadband samples. We included here only those readings taken when the ion spectra indicated that Pioneer 8 was well within or well outside of the tail, and the frequency of occurrence distributions contained in the figure are based on all appropriate observations made between January 18 and January 25. This time period was chosen to avoid biases associated with significant storm or sudden impulse encounters. (The magnetometer did detect a distinct increase in $\langle F \rangle$ and $\langle \bar{F} \rangle$ on January 20 (see Figure 1), but it appears that the electric field detector and the plasma probe both failed to respond to this particular disturbance.)

The results shown in Figure 3 vividly demonstrate that the broadband electric field characteristics within the geomagnetic tail differ significantly from those measured during quiet periods between tail crossings. Although the total number of data points is relatively small because the broadband channels are sampled at a low rate, it is clear that the occurrence distributions and the cumulative percentages have statistically significant changes that are well correlated with local changes in the positive ion spectra (the gap in $N(\phi)$ between $\phi = 8$ and $\phi = 8.5$ mv is associated with a finite digitization interval, and this is not a statistical anomaly). Before speculating on the physical mechanism that leads to this tail-associated change in the plasma wave spectrum, we will discuss the 400-Hz channel observations.

The 400-Hz Observations

The 400-Hz channel has a very well-defined 15% frequency bandwidth, and at the highest Pioneer bit rate the narrow band VLF potential amplitude is sampled once every 7 sec. Thus, the temporal resolution of this measurement is 64 times greater than that available from the broadband sequence, and much more meaningful frequency information is also provided. Although these features represent definite advantages, the 400-Hz measurement still has some unsatisfactory aspects. For instance, we recall that the Stanford radio propagation antenna is an unbalanced dipole, and thus the conversion from potential amplitude to electric field strength is difficult to determine with complete assurance. The effective length should not differ from a nominal 1-meter value by a gross amount, however, and a recent comparison of nearly simultaneous data from Pioneer 9 and OGO 5 supports this interpretation [*Scarf et al.*, 1970].

A second complication, present in all of the Pioneer 8 electric field measurements, has a more pronounced effect on the 400-Hz results than on the broadband data. We refer here to the spin modulation of the antenna response characteristics, described in detail by *Scarf et al.* [1968]. This modulation leads to a periodic finite amplitude ripple in the response, and the effect is most apparent when several samples are available on a scale time of seconds. The modulation is not as evident in the broadband data display because the points plotted are generally obtained by combining two successive samples. At the highest bit rate, each broadband point shown is an average of a pair of measurements made in a single 16-sec interval, and 448 sec elapse before another set of readings is taken in the same pulse height step. When this averaging process is combined with the long period between sampling in a given step, it is found that fine details (such as the modulation effect) are no longer visible.

The narrow 60-Hz bandwidth leads to great sensitivity with respect to variations in the ambient plasma wave spectrum, and it is appropriate to plot the 400-Hz channel data in a logarithmic format. Accordingly, the hourly maximum-minimum readings during the period January 18–31 for the two sets of low-frequency field data are displayed in different ways in Figure 4. We also show here the *Ap* values, and the percent of time plot is derived from the plasma probe spectral analysis by using the criteria discussed earlier. The 400-Hz characteristics shown in Figure 4 superficially appear to differ significantly from the broadband response curves, but it can be determined that a number of important features are quite similar. For instance, when the *minimum* values for the 400-Hz channel are compared with the broadband observations, it becomes clear that these two diagnostics have correlated responses. The storm noise enhancement extending from just before 2100 UT on January 26 to about 1130 UT on January 27 and the one commencing early on January 31 both appear clearly in the two sets of data. Similarly, many of the broadband noise minima (for instance, those on January 19, 22, 23, 24, etc.) are detected during hours when the 400-Hz minimum is also extremely low. It is obvious from Figure 4, however, that the 400-Hz maxima are extremely variable and frequently quite high during peri-

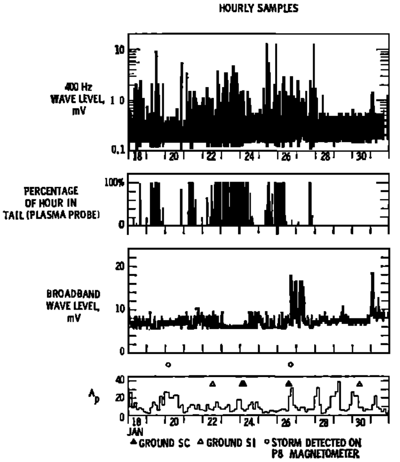

Fig. 4. Comparison of 400-Hz maximum and minimum potential amplitudes with other tail-crossing indicators. The 400-Hz output is sampled every 7 sec, and there are 64 measurements for each broadband data point. The large 400-Hz enhancements generally represent only one or two of the set of 64, and the 400-Hz averages vary in a way that resembles the minimum value shown in the top panel. Mean values for part of January 22 are collected in Table 1.

TABLE 1

	In-tail	Out-of-tail
Average broadband ϕ, mv	5.82	7.32
Average 400 Hz ϕ, mv	0.23	0.26
Minimum broadband ϕ, mv	5.55	6.30
Minimum 400 Hz ϕ, mv	0.12	0.15

ods when the broadband output is steady.

Detailed analysis of these electric field observations shows that the disparity in appearance of the two data collections is almost entirely associated with the difference in sampling rates. In essentially every case, the high values shown for the 400-Hz maximum are derived from one or two isolated enhancements in the group of 64 readings obtained while a single broadband average is acquired. If we focus attention on the mean potential amplitude over 7.46 min, we find great similarity in the variations of the 64-point 400-Hz averages and the changes in the 2-point broadband values. To demonstrate this, we show in Table 1 the range of average and minimum values for the broadband and 400-Hz potential amplitudes during the period 1700–2200 UT, on January 22. These values are separately tabulated for in-tail and out-of-tail points, and it can be seen that the 400-Hz average and minimum values also drop when Pioneer 8 is within the extended geomagnetic tail.

The 400-Hz averages generally remain fairly close to the minimum values, and the large enhancements shown in Figure 4 are thus associated with exceptional observations. In the 7 sec between 400-Hz samples, the solar wind normally travels some 2500–3500 km, and perhaps these observations of sporadic and isolated increases may simply be explained in terms of the scale sizes for the interaction regions. Because the events are rarely detected, we may assume that the disturbed regions have characteristic lengths small compared with 2000 km, with large spatial separations between isolated disturbances.

Figure 4 crudely shows that the large 400-Hz values are most frequently found in regions where plasma probe tail spectra are also observed. There are no such sporadic enhancements on January 20, 28, 29, or 30, and according to the central panel, the spacecraft was not in the tail on these days. More detailed examination of the data suggests that the 400-Hz E field enhancements are generated very near to plasma boundary regions or in places where the magnetic field gradients are high. Characteristics of the first type of boundary are illustrated

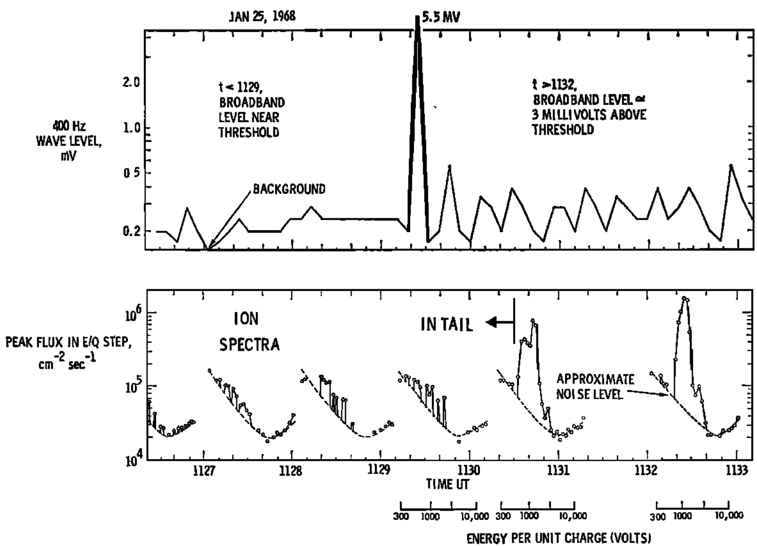

Fig. 5. An example of a tail boundary crossing with an intense 400-Hz enhancement. The peak flux at the bottom represents the largest value regardless of angle, and the plasma data are shown in sequence corresponding to the time when the measurements were made. Isolated E field enhancements of this type were frequently observed near plasma boundaries or sub-boundaries represented by steep flux or velocity gradients.

in Figure 5. The flux versus energy spectra are displayed in sequence, corresponding to the time when the measurements were taken, and the 'peak flux' connotation here means peak without regard to direction of arrival (i.e., the response in each of the 24 azimuth sectors and in each of the 3 polar-angle collectors is examined for a given E/Q value, and the largest individual flux reading is displayed). It can be seen that for $t \lesssim 1130$ UT on January 25, the individual peak flux values were so low that the plasma was virtually undetectable, whereas for $t \gtrsim$ 1130:30 UT streaming plasma with very low density and a non-Maxwellian spectrum could be detected. As described above, the criterion used to distinguish between in-tail and out-of-tail spectra gave a crossing near 1131 UT, but an actual boundary crossing near 1129:20 could easily be reconciled with these observations.

In several ways, the 400-Hz response shown here is fairly typical of that seen near many tail boundary crossings. The average potential amplitude before 1129 was slightly lower than the average value past 1130, consistent with the results shown in Table 1. It is also clear that the large 5.5-mv enhancement was singular and that the overall average for these 57 points was more than an order of magnitude below the isolated peak value. Finally, Figure 5 shows another characteristic aspect of these boundary crossings; the spin modulation customarily present in the solar wind (see *Scarf et al.* [1968]) is frequently absent near the inner edge of the tail boundary. This change can be related to a shift in spacecraft potential, perhaps associated with the presence of energetic electrons.

Figure 6 shows 1-min accumulations of 400-Hz max-min values, for a 5-hour period that contained a large number of tail crossings. The magnetic field data are scaled from Figure 8 of *Mariani and Ness* [1969], and the horizontal lines, labeled T, are the points designated as tail in the GSFC report. The horizontal lines labeled T^* near the top of the figure show where the plasma probe spectral analysis indicates that the tail is encountered. It can be seen that there is generally poor agreement between these designations. A likely explanation is that the criteria used by the magnetometer experimenters are not uniquely associated with a tail configuration. Interplanetary magnetometers detect periods of low noise with relatively high field strength and

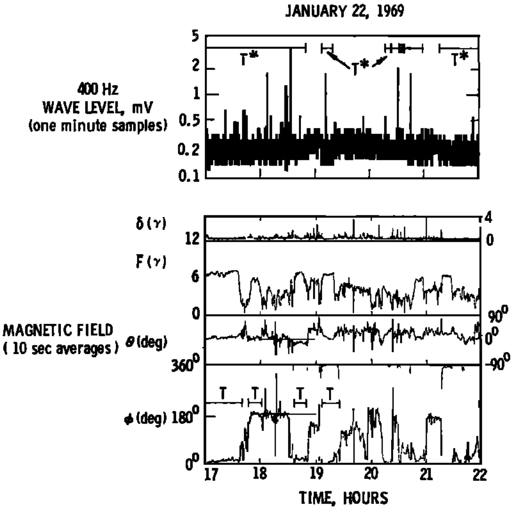

Fig. 6. Comparison of 1-min 400-Hz maximum and minimum samples (see Table 1 for averages), with 10-sec averages of magnetometer data (taken from the report by *Mariani and Ness* [1969]). The bars marked with T were designated as in-tail by the magnetometer experimenters, while those marked with T^* were judged to be in the tail on the basis of the plasma probe spectral analysis. Of the fifteen separate 400-Hz enhancements with $\phi > 500$ μv shown here, three (the first at 1725 UT, the ninth at 1842 UT, and the tenth at 1915 UT) appear to be associated with plasma probe sub-boundaries of the type shown in Figure 5. The other twelve enhancements occurred near steep gradients in $\langle F \rangle$, and these gradients were generally accompanied by field rotations.

solar or anti-solar field orientation. In addition, it now appears that the field orientation can differ from the solar or anti-solar direction when the spacecraft is within the extended geomagnetic tail.

The plasma probe tail observations designated by T^* are generally well correlated with detection of reduced minima in the 400-Hz samples, but, as in the comparison with broadband amplitudes, there are certainly some discrepancies. Here again we have a disparity in sampling rates (eight 400-Hz readings per plasma probe scan), and this fact (with the E field spin modulation) may account for much of the disagreement. Nevertheless, if we examine tail crossings such as the one near 1905 to 1920, it is clear that the plasma probe determination (T^*) is in much better agreement with the observation of a reduced E field minimum than it is with any of the bars marked by T symbols.

The 400-Hz maxima of Figure 6 show many impulsive enhancements, and there are 15 separate intervals with $\phi(\max) > 500$ μv. In 12 of these cases (all except the first at 1725, the ninth at 1840, and the tenth at 1915) the large electric field bursts are detected near specific magnetic features, where the field magnitude abruptly drops to a very low value. These dips in $|\mathbf{B}|$ also clearly define layers separating regions with different field orientations. Although the magnetometer data shown here involve 10-sec averages that tend to smear out the finest details, there is still a definite suggestion that at least twelve of these large amplitude 400-Hz readings were observed near current sheet crossings, possibly associated with X-type nulls. Because the E field is sampled only once per 7 sec, a complete correlation study is not possible on Pioneer 8. In the vast majority of cases where data could be compared, however, we have indeed found that the isolated E field maxima were detected near large depressions in $|\mathbf{B}|$ with the largest E values occurring near the maximum field gradients.

Three of the fifteen isolated enhancements shown in Figure 6 appear to be associated with plasma sub-boundaries, rather than steep magnetic field gradients and rotations. For instance, although the entire period from 1700 to about 1845 was judged to be tail-like on the basis of the plasma probe data, definite structural changes were observable within the tail. Near 1725 a brief burst of very low-density streaming plamsa [j(peak) $\simeq 2 \times 10^5$ cm^{-2} sec^{-1}, u(peak) $\simeq$ 400 km/sec] was detected, and near 1840 a non-Maxwellian spectrum with j(peak) $\simeq 4 \times 10^4$ cm^{-2} sec^{-1}, u(peak) $\simeq$ 800 km/sec was indicated, but the currents were so low that the readings were very near background. Similarly, at 1915 there was a suggestion that some flux of nonthermal plasma was present, but here the readings were so near threshold that no reliable velocities could be deduced. These three cases are apparently similar to the one shown in Figure 5, where the isolated enhancement is associated with a gradient in some plasma parameter, rather than with a current sheet crossing.

In summary, certain features of the 400-Hz channel data are clearly consistent with the broadband data in the extended tail region. For both measurements, the average and minimum response is characteristically lower than ambient in the regions where the plasma probe spectral analysis suggests that the tail is encountered. Analysis of the 400-Hz output reveals certain additional tail-associated features, presumably because much greater temporal resolution is available for this measurement. In particular, we note that isolated E field enhancements were frequently detected near plasma flux sub-boundaries or near apparent field nulls associated with rotations.

Discussion

It is difficult to identify VLF wave modes using only the Pioneer 8 electric field data because little spectral information is obtained from the single 400-Hz narrow band channel and the qualitative broadband pulseheight analysis. However, a number of supplementary arguments strongly suggest that ion sound waves or other density-related electrostatic modes are generally measured in these channels. Before summarizing these positive points, let us briefly consider the possibility that electron whistlers have been detected.

For the 1700–2200 period of January 22, the field magnitude shown in Figure 6 ranged from about 2 to about 6 γ, and the electron cyclotron frequency, f_{ce}, therefore varied from about 56 to 170 Hz. Any whistler mode waves would have $f \lesssim f_{ce}$ in the rest frame of the plasma, but because some of these waves have phase speeds (u) comparable with or smaller than V, the wind speed past the spacecraft, Doppler shift effects must be considered. The largest Doppler shift occurs for $\mathbf{u}$ anti-parallel to $\mathbf{V}$, and in this case the measured wave frequency (f') is related to the whistler mode frequency (f), by

$$\frac{f'}{Xf_{ce}} = 1 + \frac{V}{u} \tag{1}$$

Here X is defined by $f = Xf_{ce}$.

For the enhancements detected near 1815–1845 UT on January 22, we set $f_{ce} = 84$ Hz ($\langle F \rangle \simeq 3\gamma$), $V = 600$ km/sec (see Figure 1), and $f' = 400$ Hz. Then if $X \simeq 1$, we must have $u \simeq 155$ km/sec for f' to appear at 400 Hz, but if X is as small as 0.5, we need $u \simeq 70$ km/sec. These extremely small phase speeds imply that the index of refraction n is very large, and this in turn means that the electric amplitude in the hypothetical whistler mode wave is small compared with the magnetic component, because E and B are related by

$$E = \frac{cB}{n} = uB \qquad (2)$$

This point alone makes it extremely unlikely that whistler mode waves are represented by any of these observations. In the disturbed magnetosheath of the earth, the normal magnetic noise level developed in a 15% bandwidth filter channel centered at 400 Hz is about 1 mγ [*Scarf et al.*, 1968; *Smith et al.*, 1967], and for $u \simeq 155$ km/sec, equation 2 then predicts an electric magnitude of 0.15 μv/meter. The observed 400-Hz enhancements are thus frequently factors of 10^4 greater than what might be expected using equation 2 and normal VLF magnetic amplitudes. Even for the most intense sporadic high-frequency noise bursts detected in the magnetosheath, the peak magnetic amplitudes of about 10^{-1} γ [*Smith et al.*, 1969] would only lead to $E(\max) \simeq 15$ μv/meter, and this is still well below the peaks shown in Figure 6.

There are other strong reasons for discarding the hypothetical whistler mode identification. If we were detecting right-hand polarized electromagnetic waves, then n^2 would be given by

$$n^2 = \frac{c^2}{u^2} \simeq \frac{f_{pe}^{\ 2}}{f_{ce}^{\ 2} X(1 - X)} \qquad (3)$$

where $f_{pe} = 9 \times 10^3\ (N)^{1/2}$ Hz is the electron plasma frequency, and N is the density in cm^{-3}. For $u = 155$ km/sec and $n \simeq 2000$, equation 3 can readily be solved for X as a function of N. One finds $X = 1 - \epsilon$, with $\epsilon \simeq 3 \times 10^{-3} N$, and any reasonable density (e.g., $N \simeq 1$) gives $\epsilon \ll 1$ or $f \simeq f_{ce}$. For a warm plasma such as the solar wind, however, electron whistlers with

$$(f_{ce} - f) \lesssim f(\kappa T/m)_-^{1/2}/u \qquad (4)$$

are very heavily damped, and they cannot propagate [*Stix*, 1962]. Because $(\kappa T/m)^{1/2}$ is certainly greater than 155 km/sec for the local electron distributions in the wind and extended tail, we can therefore ignore the whistler mode conjecture on this basis as well.

Electrostatic ion modes have wave frequencies related to the ion plasma frequency [$f_{p+} \simeq 210(N)^{1/2}$ Hz for protons], and phase speeds are comparable with $(\kappa T_+/m_+)^{1/2}$. Thus, Doppler shifts must again be considered when these modes are examined, and for $N \simeq 0.1$–10 one might expect to detect ion sound waves in the broadband analysis ($f \geq 100$ Hz) or in the 400-Hz channel. Because low broadband response and decreased 400-Hz minima are both found where the plasma probe indicates that Pioneer 8 is within the tail, one might consider that the tail density is very low, that tail Doppler shifts are somehow minimized, or that both phenomena contribute to the observations. However, detailed examination of the data suggests that only the first of these possibilities is likely.

The wake region between tail crossings contains a plasma with markedly reduced flux values [*Siscoe et al.*, 1970*a*], and it appears from study of the energy spectra that a major part of this reduction is associated with a decrease in density, rather than an increase in temperature. The individual tail spectra are frequently so non-Maxwellian that it is not possible to deduce local plasma parameters for most in-tail periods. The plasma probe criteria summarized in the second section do not select spectra with low streaming speeds, however, and for many of the periods designated as tail the plasma velocity was comparable with that found in the surrounding regions. Thus, it is difficult to attribute the in-tail decrease in E field levels to a reduction of Doppler shifting. On the other hand, the in-tail criteria are generally quite consistent with detection of an extremely low plasma density. Because a change in N from 1 to 0.1 cm^{-3}, for example, would produce a decrease in f_{p+} from 210 to about 67 Hz, it is plausible to expect that a broadband channel measuring only waves with $f \geq 100$ Hz could have a background response inside the tail, as suggested by the data of Figures 1, 2, and 3. (We do not seriously consider that the in-tail region is quiet for all frequencies because the plasma spectra are very non-Maxwellian here.)

The general correlation between mean potential amplitude levels (broadband and 400 Hz) and ambient solar wind density has been established independently by using non-tail data from Pioneer 8 and nearly simultaneous undisturbed plasma probe observations from Explorer 35 [*Siscoe et al.*, 1970*b*]. The joint results are consistent with an interpretation that the average or mean VLF electric field noise levels in the wind decrease with increasing frequency, and that the spectral width is related to f_{p+}. (The OGO 5 plasma wave experiment also makes electric field observations in the solar wind over the range 200 Hz to 70 kHz [*Crook et al.*, 1969]. Very preliminary studies of low-level interplanetary E field spectra from OGO 5 support the above interpretation of spectral shape, but at present the quiet-time analysis has not been carried out in detail.)

The sporadic enhancements observed in the 400-Hz channel indicate that different plasma wave spectra are encountered near steep gradients in $\langle F \rangle$, when these dips are associated with field rotations. Very similar phenomena have been observed on Pioneer 9 and on OGO 5 [*Scarf et al.*, 1969], especially in the magnetosheath. The OGO experiment has excellent temporal resolution, because an E field digital sample is obtained every 144 msec at the 8 kbit/sec telemetry rate, and analog E field waveforms for 1 kHz $< f <$ 22 kHz are transmitted on the special purpose telemetry. It is useful, therefore, to examine OGO 5 data in the region of similar current sheet crossings, and Figure 7 shows relevant particle, field, and wave characteristics observed when OGO 5 was in the magnetosheath on April 5, 1968. The very abrupt dips in field magnitude occurred at field rotational boundaries [*Scarf et al.*, 1969]; the ion spectrometer data (courtesy of Dr. G. Sharp) and the Langmuir probe observations (courtesy of Dr. K. Norman) showed that the particle distributions in these regions were highly variable over very short times (fractions of seconds) and that they were not Maxwellian. The largest electric field enhancements were found near the steepest gradients in field strength, and the electrostatic levels changed by orders of magnitude in very short times.

The OGO 5 observations suggest that the currents producing the field nulls at rotational boundaries are large enough to trigger 2-stream instabilities that generate ion sound waves. The smallest scale lengths for the interaction regions are comparable to those found in the collisionless bow shock [*Fredricks et al.*, 1968], and the relationship between electrostatic wave amplitude and B field gradient is also similar to that commonly found in the shock.

Because the Pioneer 8 E field experiment is so limited, we cannot be certain that the configurations shown in Figure 6 resemble the ones displayed in Figure 7. However, it is tempting to speculate that B field dips and 400-Hz

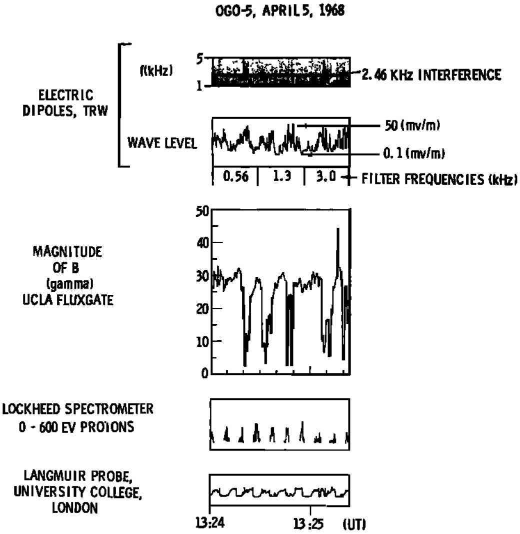

Fig. 7. Characteristics of X-type nulls detected when OGO 5 was in the magnetosheath. The particle data indicated that the distributions were non-Maxwellian and that rapid temporal variations were occurring. The sharp dips in magnetic field strength were accompanied by rotations, and the electrostatic noise bursts had maximum amplitudes where the field gradients were steepest.

enhancements found on Pioneer 8 are associated with field line merging or reconnection in the extended geomagnetic tail. The skewed B field on the two sides of a 'null' will tend to merge according to Maxwell's equations,

$$\nabla^2 B = \mu_0 \sigma \frac{\partial B}{\partial t} \tag{5}$$

where σ is the conductivity in mks units. The merging time (τ) depends on the overall scale length (L) and $\tau \simeq \mu_0 \sigma L^2$. If Coulomb collisions were to provide the only mechanism for a finite conductivity, then we might consider the use of

$$\sigma(\text{coulomb}) \simeq 6.3 \times 10^{-4} T^{3/2} (\text{ohm meter})^{-1} \tag{6}$$

where T is in degrees Kelvin [*Spitzer*, 1962]. If $T \simeq 10^5$ °K, then $\sigma(\text{coulomb}) \simeq 2 \times 10^4$/ohm meter, and for $L \simeq 100$ km, for instance, we find $\tau(\text{coulomb}) \simeq 2.5 \times 10^8$ sec. This illustrates the inefficiency of coulomb collisions in providing a dissipation mechanism for the solar wind plasma, and we conclude that these binary interactions cannot produce meaningful reconnection.

However, several processes can lead to greatly enhanced resistivity and dissipation in a collisionless plasma. As discussed by *Speiser* [1970], an effective conductivity can be defined when the characteristic system length is small. Accelerated particles carry energy away, and there is effective local dissipation without collisions or noise. Another resistive mechanism involves scattering of particles by locally generated waves. Laboratory experiments [*Bratenahl and Yeates*, 1970] show that the onset of field annihilation in a confined system is correlated with the appearance of intense plasma turbulence.

If individual particles interact with organized groups of particles or waves, then the conductivity is

$$\sigma(\text{wave}) = \frac{Ne^2}{m_e\nu}(\text{ohm meter})^{-1} \qquad (7)$$

where N, e, and m are in mks units, and ν is the effective wave-particle 'collision time.' *Sagdeev* [1958], *Kadomtsev* [1965], and *Fredricks* [1969] have estimated that ion sound waves lead to $\nu \simeq 0.1\ \omega_{p+} = 0.628\ f_{p+}$. For $N = 1$ $\text{cm}^{-3} = 10^6\ \text{m}^{-3}$, equation 7 then gives σ(ion wave) $\simeq 2\times 10^{-4}$/ohm meter, and for $L \simeq$ 100 km, the merging time is drastically reduced to about 2–3 sec.

These numerical estimates of σ, L, and τ are, of course, essentially qualitative, but the physical result is highly significant. If current instabilities at X-type nulls do develop large amplitude ion sound waves, then the wave-particle scattering provides a dissipation mechanism that allows field line merging or reconnection to occur. The sparse evidence obtained by the Pioneer 8 electric field experiment suggests that a sequence of events leading to tail breakup does in fact occur at $r \simeq$ 500–800 R_E, with ion sound waves providing a physical dissipation process for reconnection. It is hoped that future probes traversing the extended geomagnetic tail region will carry more complete wave experiments to explore this phenomenon in greater detail, and that coverage will also be extended to the region within 500 R_E.

Acknowledgments. We thank E. W. Greenstadt for his assistance with some preliminary statistical studies and R. W. Fredricks, T. W. Speiser, and C. M. Yeates for helpful discussions concerning anomalous plasma conductivity. We are indebted to P. J. Coleman, Jr. and C. T. Russell for furnishing the magnetometer data used in Figure 7, and we are also grateful to G. W. Sharp and K. Norman for permitting us to display some simultaneous particle characteristics. The invaluable assistance of A. Cowen and H. Collard in processing and analyzing the large amount of data is gratefully acknowledged.

The primary support for this research was supplied by the National Aeronautics and Space Administration under Contract NAS 2-4673.

The Editor wishes to thank Dr. B. U. Ö. Sonnerup and Dr. T. W. Speiser for their assistance in evaluating this paper.

REFERENCES

Axford, W. I., The interaction between the solar wind and the magnetosphere, in *Physics of Geomagnetic Phenomena,* edited by S. Matsushita and W. H. Campbell, p. 1243, Academic Press, New York and London, 1967.

Bratenahl, A., and C. M. Yeates, Experimental study of magnetic flux transfer at the hyperbolic neutral point, *Phys. Fluids,* in press, 1970.

Crook, G. M., F. L. Scarf, R. W. Fredricks, I. M. Green, and P. Lukas, The OGO-5 plasma wave detector: instrumentation and in-flight operation, *IEEE Trans. Geosci. Electron., GE-7, 2,* 120, 1969.

Dungey, J. W., Damping of waves in the current sheet in the geomagnetic tail by radiation, *Planet. Space Sci., 17,* 1291, 1969.

Dungey, J. W., and T. W. Speiser, Electromagnetic noise in the current sheet in the geomagnetic tail, *Planet. Space Sci., 17,* 1285, 1969.

Fredricks, R. W., Electrostatic heating of solar wind ions beyond 0.1 AU, *J. Geophys. Res., 74,* 2919, 1969.

Fredricks, R. W., C. F. Kennel, F. L. Scarf, G. M. Crook, and I. M. Green, Detection of electric-field turbulence in the earth's bow shock, *Phys. Rev. Lett., 21,* 1761, 1968.

Intriligator, D. S., J. H. Wolfe, D. D. McKibbin, and H. R. Collard, Preliminary comparison of solar wind plasma observations in the geomagnetospheric wake at 1000 and 500 earth radii, *Planet. Space Sci., 17,* 321, 1969.

Kadomtsev, B. B., *Plasma Turbulence,* Academic Press, New York, 1965.

Mariani, F., and N. F. Ness, Observations of the geomagnetic tail at 500 earth radii by Pioneer 8, *J. Geophys. Res., 74,* 5633, 1969.

Ness, N. F., C. S. Scearce, and S. Cantarano, Probable observations of the geomagnetic tail at 10^3 R_E by Pioneer 7, *J. Geophys. Res., 72,* 3769, 1967.

Sagdeev, R. Z., *Plasma Physics and Problems of Controlled Thermonuclear Reactions,* Vol. 4, p. 454, Moscow, USSR, 1968.

Scarf, F. L., Interplanetary waves and their effects on the magnetosphere, *Proc. 16th URSI General Assembly,* Ottawa, Canada, 1969.

Scarf, F. L., G. M. Crook, I. M. Green, and P. F. Virobik, Initial results of the Pioneer 8 VLF electric field experiment, *J. Geophys. Res.*, *73*, 6665, 1968.

Scarf, F. L., P. J. Coleman, Jr., R. W. Fredricks, C. F. Kennel, and C. T. Russell, Magnetic and electric field changes across the shock and in the magnetosheath, *Proc. Third ESLAB/ESRIN Symposium on Intercorrelated Satellite Observations,* Noordwijk, Holland, 1969.

Scarf, F. L., C. F. Kennel, R. W. Fredricks, I. M. Green, and G. M. Crook, AC fields and wave particle interactions, in *Earth's Particles and Fields, 1969,* edited by B. M. McCormac, Reinhold Publishing Company, New York, 1970.

Siscoe, G. L., F. L. Scarf, D. Intriligator, J. H. Wolfe, J. H. Binsack, H. S. Bridge, and V. M. Vasyiliunas, Evidence for a geomagnetic wake at 500 R_E, submitted to *J. Geophys. Res.*, 1970*a*.

Siscoe, G. L., F. L. Scarf, I. M. Green, J. H. Binsack, and H. S. Bridge, VLF electric fields in the interplanetary medium: Pioneer 8, to be submitted to *J. Geophys. Res.*, 1970*b*.

Smith, E. J., R. E. Holzer, M. G. McLeod, and C. T. Russell, Magnetic noise in the magnetosheath in the frequency range 3–300 Hz, *J. Geophys. Res.*, *72*, 4803, 1967.

Smith, E. J., R. E. Holzer, and C. T. Russell, Magnetic emissions in the magnetosheath at frequencies near 100 Hz, *J. Geophys. Res.*, *74*, 3027, 1969.

Speiser, T. W., Conductivity without collisions or noise, *Planet. Space Sci.*, in press, 1970.

Spitzer, L., Jr., *Physics of Fully Ionized Gases,* Interscience, New York, 1962.

Stix, T. H., *The Theory of Plasma Waves,* McGraw-Hill, New York, 1962.

Wilcox, J. M., and D. S. Colburn, Interplanetary sector structure in the rising portion of the sunspot cycle, *J. Geophys. Res.*, *74*, 2388, 1969.

Wolfe, J. H., R. W. Silva, D. D. McKibbin, and R. H. Mason, Preliminary observations of a geomagnetic wake at 1000 earth radii, *J. Geophys. Res.*, *72*, 4577, 1967.

(Received December 31, 1969;
revised February 12, 1970.)